



ICEECIT
International Conference on Electrical Engineering,
Computer and Information Technology

2022 International Conference on Electrical Engineering, Computer and Information Technology (ICEECIT) | 978-1-6654-9352-9/\$22/\$31.00 ©2022 IEEE | DOI: 10.1109/ICEECIT55908.2022.10030497



ICEECIT 2022 PROCEEDINGS

2022 International Conference on Electrical
Engineering, Computer and Information Technology
(ICEECIT)

Sponsorship:



**November
22th - 23th, 2022
Universitas Jember**

<https://iceecit.unej.ac.id/>

Table of Content	Pages
Optimization of Random Forest with Genetic Algorithm for Determination of Assessment	1-6
Feature Selection Application to Classify Medicinal Plant Leaves using LVQ	7-13
Attractive Learning Media for Introduction to Popular Fruits Using Computer Vision	14-19
Chronic Kidney Disease Severity Identification Using Template Matching Feature Selection Statistics Based	20-24
Hotel Review Sentiment Analysis Using Indonesian Language Based Machine Learning	25-28
Comparison of Classification Algorithm to Determine Potential Fishing Area Based on Coral Reefs	29-33
A New Approach Puch and Kick Identification in Martial Sport Pencak Silat using Fuzzy Logic	34-38
Optimization Silhouette Coefficient on Genetic Algorithm for Clustering	39-43
Comparison of Classification Methods Using Feature Selection for Smartphone Sentiment Analysis	44-48
Time-Series Analysis of Cryptocurrency Price: Bitcoin as a Case Study	49-53
Detection Of Road Damage Using Faster Regional-Convolutional Neural Network Method	54-59
Lane Departure Warning based on Road Marking Detection using Mask R-CNN	60-64
Implementation of the K-means clustering for the Public Health Center data	65-69
Implementation Goalkeeper Robot's Movement Response With Odometry Use PID Method	70-75
A Robust Visual-IMU-Wheel Odometry Using PID Controller for Autonomous Soccer Robots	76-81
Fuzzy Logic Control-Based Interleaved Boost Converter for Proton Exchange Membrane Fuel Cell System Applications	82-87
PID Control Design and Kinematic Modelling of 3-DoF Robot Manipulator	88-94
Vessel Monitoring Application Using Automatic Identification System Data	95-98
Design a Smartphone App of an Internet Of Things-Based Monitoring System Potato Plants on Agricultural Land	99-103

Table of Content	Pages
Temperature Characteristics of 10nm N- and P-Channel Si-FinFET structure	104-107
Prediction of LED Arrangement Illumination on Street Light Armature Using Random Forest Regression Method	108-112
Interfacing PCI 1710 with Real Time Windows Target for Induction Motor Speed Control Based on Vector Control designed by Variable Flux Reference	113-117
Daily Power Plant Load Prediction using Grammatical Evolution	118-122
Design of a Dynamometer as a Measuring Tool for Power Efficiency and Performance Characteristics of a Brushless DC Motors	123-130
Early Warning System Design for Flood Disasters Using the IoT-Based Fuzzy Logic Control Method	131-135
Inverter Design With Selective Harmonic Elimination Pulse Width Modulation (SHE PWM) Method For Agricultural Irrigation Pump	136-140
Prototype Control of DC-DC Boost Converter in Solar Cell Energy Management System Based on Fuzzy Logic Method	141-148
Global Horizontal Irradiance Forecasting Using Hybrid method: Convolutional Neural Network-Long Short Term Memory	149-152
Implementation of Monitoring Device for Fault Location, Isolation, and Service Restoration (FLISR) in Jakarta Area Distribution Network	153-158
Analysis Of Protection System Based On-Line Current Differential Using Nominal Phi Method On 150 Kv Transmission Line Ngimbang-Babat 1	159-166
Prediction and Gaussian Distribution Analysis of Power Consuming in University Building Using BiLSTM Deep Learning	167-173
Impact of DFIG Inertia on Short Circuit Fault Current Components	174-178
Analysis Of 500 Ohm Neutral Grounding Resistance (NGR) Grounding System On A 60 MVA Power Transformer Of One Phase To Ground Faults At The Banyuwangi 150 kV Substation	179-186
K-means algorithm to identify the optimal production period of a photovoltaic array installed at any point in a very large area	187-192
Non-Intrusive Load Monitoring Based on Advanced-Boosting Algorithm	193-198
Dynamic voltage stability study of a stand-alone photovoltaic microgrid supplying an electric mill in Benin rural zone	199-204
Analysis of DCO OFDM Application in MIMO NOMA VLC System Serving 8 Users	205-208

Table of Content	Pages
Implementation of a 3D Indoor Positioning System Using MLP based Distance Estimation for IoT Applications	209-214
Prototype of Building Monitoring System Using Vibration Sensor Based on Wireless Sensor Network	215-221
LoRa SNR Evaluation as Portable Sensor	222-225
Parameters Quality Performance of Signal Fluctuation Based on Data Grouping	226-231
Design Of Wireless Sensor Network (WSN) System Using Point To Point And Waiting Protocol Methods For Solar Panel Monitoring	232-240
Fuzzy Logic Controlled Sepic Converter System For 36 W Vertical Wind Turbine Performance Improvement	241-246
Regenerative Braking Using Fuzzy Logic Control on BLDC Motor Driven Electric Vehicles	247-252
Reliability Index Evaluation of Distribution System Using Section Technique Method at Penyulang Watu Ulo PT. PLN UP3 Jember ULP Ambulu	253-257
Emission Impact between Coal Fired and Renewable Energy Power Plant Development: Evidence from Indonesia	258-261
Improving The Stability of Sulselrabar System with Dual Input Power System Stabilizer Based On Imperialist Competitive Algorithm	262-267
Fault Prediction in Photovoltaic Systems with Extreme Learning Machine Modeling	268-273
Monitoring and Controlling Overfeeding Ammonia in Smart Lobster Ponds based on Internet of Things Technology	274-279



IEEE Conference Number # 55908

Copyright and Reprint Permission.

Abstracting is permitted with credit to the source. Libraries are permitted to photocopy beyond the limit of U.S. copyright law, for private use of patrons, those articles in this volume that carry a code at the bottom of the first page, provided that the per-copy fee indicated in the code is paid through the Copyright Clearance Center, 222 Rosewood Drive, Danvers, MA 01923. For copying, reprint, or reproduction requests should be addressed to IEEE Copyrights Manager at pubs-permissions@ieee.org.

IEEE Catalog Number Part Number CFP22CV2-ART

ISBN 978-1-6654-9352-9

AUTHOR INDEX

A Sumarudin
Abdelhafid Tobbal
Abdelmoughni Toubal
Abdul Madjid
Abdullah Syah
Achmad Danil Endrico
Adi Suheryadi
Adinda Ayu Triasasti
Adri Senen
Agus Setiawan
Ahmad Firyal Adila
Ahmad R. H. Tahier
Aji Wahyu Prasetyo
Akmalul Fata
Ali Rizal Chaidir
Amevi Acakpovi
Andi Junaidi
Andi Kurniawan
Andi Tejawati
Andrita Ceriana Eska
Anindita Septiarini
Arionmaro Simaremare
Arizal Mujibtamala Nanda Imron
Assaidah Assaidah
Atthariq Atthariq
Aulia Istiqomah
Avip Zain Haq
Azam Zamhuri Fuadi
Bagas Satya Dian Nugraha
Bambang Kaloko
Bambang Sujanarko
Billel Bengherbia
Burhan Kholis
Chao-Rong Chen
Cossi Téséphore Nounangnonhou
Cyriaque Bosco Mitokpe
Dedy Kurnia Setiawan
Dedy Wahyu Herdiyanto
Devita Ayu Larasati
Dewandy Des Ramadhana
Dezetty Monika
Dhani N.I Syamputra
Djoko Saryono

Dodi Setiabudi
Eko Mulyanto Yuniarno
Eko Noerhayati
Era Purwanto
Erika Fiqrilinia
Faaris Mujaahid
Fitri Anik
François Xavier Nicolas Fifatin
Gamma Aditya Rahardi
Ghiyalti Novilia
Gigih Prabowo
Ginas Alvianingsih
Guido Kalandro
Hamdani Hamdani
Hamza Hentabli
Hari Putranto
Harun Ismail
Haryanto Haryanto
Hasanur Mohammad Firdausi
Hasna Satya Dini
Herri Akhmad Bukhori
Ian Jack Permana
Ifan Prihandi
Ilham Ramadani Arianto
Imam Robandi
Immawan Wicaksono
Indra Ardhanayudha Aditya
Indra Ferdiansyah
Indra Ranggadara
Inung Wijayanto
Irawan Dwi Wahyono
Jangkung Raharjo
Joseph Cahya Putra
Karisma Putra
Katherin Indriawati
Khoirudin Asfani
Kossoko Babatoundé Audace Didavi
Lalitya Nindita Sahenda
Lamidi Taohidi Alamou
Langlang Gumilar
Lilik Anifah
Lisa Yihaa Roodhiyah
Luthfansyah Mohammad
Macaire Agbomahena

Mahmoud Elsis
Mamat Rokhmat
Masna Wati
Melinda Melinda
Moch Syaiful Komar
Mochammad Alif Naufal Yafi
Mochammad Fahrizal Firdaus
Moh. Iskandar Zulkanain
Moh. Rozaq Febri Sudiby
Moh. Zainul Zainul Falah
Mohamad Agung Prawira Negara
Mohamad Rodhi Faiz
Mohamed el amine Bougheriza
Mohd Murtadha Mohamad
Mohd Nihra Haruzuan Bin Mohamad
Said
Mohd Shafie Rosli
Mounir Bouhedda
Muh Asnoer Laagu
Muh Jamil
Muhammad Irhamsyah
Muhammad Makarimal Akhlak
Muhammad Muhammad
Muhammad Ridho Rosa
Muhammad Rizani Rusli
Muhammad Ruswandi Djalal
Muhammad Sarman Noorlah
Muhammad Syariffuddien Zuhrie
Nien-Che Yang
Noor Dayana Abd Halim
Novianti Puspitasari
Nur Hafnita
Nur Holis
Nur Widi Priambodo
Nurbiha A Shukor
Nurul Zainal Fanani
Pawenary Pawenary
Qasem Abu Al-Haija
Ramzi Adriman
Rb Moch Gozali
Reza Fuad Rachmadi
Richard Agbokpanzo
Rio Irawan
Rizdky Oktaviari Pratama Putra

Rizky Nuzul Kurnianda
Rudy Rachman
Ruri Wahyuono
S Sunarti
Satriananda Satriananda
Satrio Yudho
Satryo Utomo
Soraya Ananta P
Soraya Mustika
Stieven Netanel Rumokoy
Suhendra Suhendra
Sujito Sujito
Sumardi Sumardi
Suprihadi Prasetiono
Suyanto Suyanto
Syahrial Syahrial
Syam Widiyanto
Taufik F. Abidin
Timotius Heries Noventino
Triwahju Hardianto
Wahyu Muldayani
Wawan Gunawan
Widjonarko Widjonarko
Willy Permana Putra
Yasir Hashim
Yuli Mauliza
Yunidar Yunidar
Yunita Sartika Sari
Zainal Arifin
Zeyad Albatati Action
Zilvanhisna Emka Fitri
Zul Arsil Mustofa

PREFACE TO THE CONFERENCE PROCEEDINGS

On behalf of the conference committee, first of all, I would like to thank God Almighty for holding this activity. I also extend a warm welcome to all involved in our International Conference on Electrical, Computer Technology, and Information Engineering (ICEECIT).

As the General Chair of this conference, I am honored and would like to thank those who have played a part in this important event.

First of all, I would like to thank and appreciate the leadership of the University of Jember, who has been willing to provide funds and other facilities so that this event can be held. Second, I express my gratitude and appreciation to the IEEE Indonesia Section and the Power Energy System IEEE Indonesia Section Chapter for sponsoring this activity. Third, my thanks to the reviewers that have examined the papers so that only the ones that meet the quality can be published in conferences and proceedings. Fourth, thanks to the authors, moderators, and participants for collaborating in improving science and technology. Fifth, I express my highest gratitude and appreciation to my colleagues from the organizing committee and my students for their tireless efforts in managing this conference.

I realize that organizing this first conference still has several obstacles, although my team and I have tried our best to manage it as best we can.

Finally, I hope that our conferences and proceedings that have been published can significantly contribute to the welfare of humanity.

Prof. Dr. Ir. Bmbang Sujanarko, MM, IPM
ICEECIT General Chair

Prototype Control of DC-DC Boost Converter in Solar Cell Energy Management System Based on Fuzzy Logic Method

Bambang Sri Kaloko
Electrical Engineering Major
 University of Jember
 Jember, Indonesia
 kaloko@unej.ac.id

Wahyu Muldayani
Electrical Engineering Major
 University of Jember
 Jember, Indonesia
 wahyumuldayani.teknik@unej.ac.id

Mochammad Alif Naufal Yafi
Electrical Engineering Major
 University of Jember
 Jember, Indonesia
 malifnaufalyafi@gmail.com

Andrita Ceriana Eska
Electrical Engineering Major
 University of Jember
 Jember, Indonesia
 andritacerianaeska@gmail.com

Guido Dias Kalandro
Electrical Engineering Major
 University of Jember
 Jember, Indonesia
 guidokalandro89@unej.ac.id

Muh. Asnoer Laagu
Electrical Engineering Major
 University of Jember
 Jember, Indonesia
 asnoer@unej.ac.id

Abstract—Population growth greatly affects the world's electricity consumption, so there will come a time when renewable energy is needed to be an alternative to the generation system from fossil fuels. The generation of energy derived from renewable energy requires a range of converters and storage systems. The research methodology used is to use the DC-DC boost converter topology to regulate the output voltage of the dc bus connected to a 12W DC lamp load when the photovoltaic source is unable to meet the load power demand. This research focuses on the goal of designing a DC-DC boost converter on a photovoltaic system, being able to use battery power with a DC-DC boost converter to maintain load power supply, and adjusting the PWM boost trigger using the fuzzy logic method. The DC-DC boost converter is designed with component calculations using the boost converter equation which worked well in boost mode testing with an average percent error value of 3.88%. The DC-DC boost converter system with the fuzzy logic method successfully uses batteries to maintain the load power during data retrieval, the load voltage is maintained between 13.89V to 14.06V with a power range of 9.91W to 13.73W. The fuzzy logic method implemented successfully regulates the work of declaring MOSFET boost so as to produce a voltage close to the reference voltage of 14V with a voltage range of 13.89V to 14.06V using an accumulation of PWM values with a range of values of 53.07 to 56.89.

Keywords—Boost Converter, Fuzzy, Photovoltaic, PWM

I. INTRODUCTION

The need for electrical energy in the world over time is increasing. There will come a time when humans look for other sources of energy, besides fossil energy that will one day run out and cannot be renewed. This alternative energy is needed by being driven by economic growth and population growth. This increase in growth leads to an increase in the consumption or use of electrical energy, thus requiring renewable energy sources [1].

One of the most important elements in a renewable energy system is its storage system. A battery is a component that stores chemical energy so that it can be used as electrical energy by electrochemical processes [2]. Currently, renewable energy systems that require energy storage systems are solar power plants or photovoltaic systems. The

process of generating energy fluctuations requires a series of converters. The converter circuit is needed to adjust the output of the photovoltaic system to be stable so that it can supply the load well. This converter circuit uses a DC-DC Boost Converter circuit that is capable of delivering power to supply the load when PV power is considered unable to meet the load power

Therefore, the author wants to create a DC-DC Boost Converter system that is triggered using Arduino-based PWM or Pulse Width Modulation with the Fuzzy Logic method. This DC-DC Boost Converter system aims to control the output voltage of the battery when the photovoltaic system cannot meet the load power.

II. RESEARCH METHODS

The DC-DC Boost Converter system consists of a PV or photovoltaic system as a power source along with a step-down module LM2596 as a PV source voltage level lowering equipped by a 6A diode to protect the photovoltaic system from backflow, a DC-DC Boost Converter circuit as a voltage level regulator on the DC Bus and a DC lamp as a load.

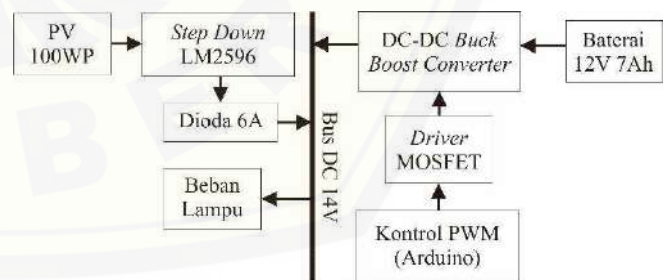


Fig 1. DC-DC Boost Converter System Diagram Block

According to Fig. 1, a PV or photovoltaic source supplies power to the DC bus via step-down buck LM2596 and diode 6A. Diode 6A is used as backflow protection from DC to PV buses. The voltage on the DC bus is set at 14V by lowering the pv source voltage level by the step-down module LM2596. The power supply from the PV source is used by a load, namely a DC lamp. A 12V 7Ah battery can act as a power supply with the help of a DC-DC boost converter. This

battery system is set up with the performance of a DC-DC boost converter that works in boost mode. This boost mode is regulated by the PWM control system of the Arduino Mega 2560 microcontroller using the fuzzy method which then regulates the work of the MOSFET with the help of the MOSFET driver.

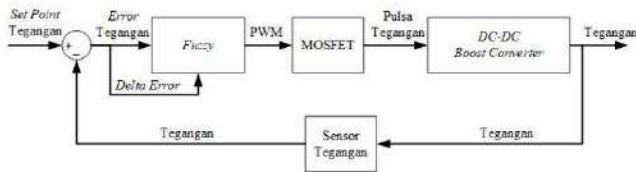


Fig 2. Converter Work Control Block

Based on the control block in Fig. 2, the system is given a set point in the form of a reference voltage of 14V which is a reference, and then a voltage error is generated from the voltage reduction of the set point with the voltage read by the voltage sensor, a delta error from the voltage error is also obtained. Both of these variables are used in fuzzy processes. It uses fuzzy rules and generates an affirmation in the form of a PWM signal that regulates the work of the MOSFET. The MOSFET generates a voltage pulse that regulates the voltage level on the DC-DC Boost Converter. This converter produces parameters in the form of a voltage that are read by the voltage sensor as feedback.

In this study, a Photovoltaic Module or Solar Module was used as specified in table I.

TABLE I. SOLAR MODULE SPECIFICATION

Module Type	MSP-100W
Cell Type	Monocrystalline Silicon
Rated Max. Power (Pmax)	100W
Current at Pmax (Imp)	5,54A
Voltage at Pmax (Vmp)	18,1V
Short-Circuit Current (Isc)	6,00A
Open-Circuit Voltage (Voc)	22.2V
Dimension (mm)	1020×670×30
Maximum System Voltage	700V
Temperature Range	-45°C to +80°C

A. Converter Design

The design and selection of components when the converter is in a boost condition, namely the calculation of the duty cycle boost, the calculation of the minimum inductor value, and the calculation of the minimum capacitor [3], as follows:

1) Duty Cycle Boost Calculation

The calculation of Duty Cycle Boost is carried out using the following equation:

$$V_o = \frac{V_{in}}{(1 - D_{boost})}$$

$$D_{boost} = 1 - \frac{12}{14}, D_{boost} \text{ max} = \frac{14 - 12}{14 - 14} = \frac{2}{14} = 0,14286$$

$$D_{boost} = 1 - \frac{9}{14}, D_{boost} \text{ min} = \frac{14 - 9}{14} = \frac{5}{14} = 0,35714$$

From the boost mode duty cycle protection above, the input voltage comes from a 12V lead acid battery with a voltage range of 9V to 12V so that two duty cycle limits are obtained, namely from 14.286% to 35.714%.

2) Calculation of Minimum Inductor Value

The calculation of the Minimum Inductor Value is carried out using the following equation:

$$L_{min} = \frac{V_{Batt} \times D_{boost}}{\Delta I \times f_s}$$

$$L_{min} = \frac{12 \times 0,14286}{0,554 \times 20 \times 10^3}$$

$$L_{min} = \frac{1,71432}{11080} = 154,722\mu H$$

From the calculation of the minimum inductor value above, the duty cycle value of the boost mode used is also the minimum duty cycle of the boost mode with a ripple current of 0.554A and the switching frequency at 20KHz resulting in a minimum inductor value of 154.722μH.

3) Calculation of Minimum Capacitor Value

The calculation of the Minimum Capacitor Value is carried out using the following equation:

$$C_2 = 2,14 \times \frac{I_o}{\Delta V} \times D_1 \times T$$

$$C_2 = 2,14 \times \frac{0,3}{1\% \times 14} \times 0,86 \times 50 \times 10^{-6}$$

$$C_2 = 197,18571398\mu F$$

The minimum capacitance value used in boost mode is determined to be equal to the minimum capacitance value in buck mode with a capacitor value of 197.18571398μF.

B. Fuzzy Method Design

This fuzzy method aims only to regulate the work of the converter in boost mode so that the converter can produce a voltage of 14V to the dc bus stably. The design of inputs and outputs of the Mamdani-type fuzzy method uses several kinds of value ranges and is based on the fuzzy rule that has been created.

1) Input Error Voltage Membership Function

Input Error Voltage is calculated from the reduction between the reference voltage which is 14V and the converter output voltage in boost mode. The membership function on the input error voltage consists of three subsets:



Fig 3. Voltage error input membership function

- N (Negative) $\mu_N E[x] : [-2 -2 0]$
- Z (Zero) $\mu_Z E[x] : [-1 0 1]$
- P (Positive) $\mu_P E[x] : [0 2 2]$

2) Input Membership Function Delta Error Voltage

Input Delta Error Voltage is obtained from the reduction between the output voltage of the previous converter (n-1) and the current output voltage (n). The membership function on the input delta error voltage consists of three subsets, as follows:

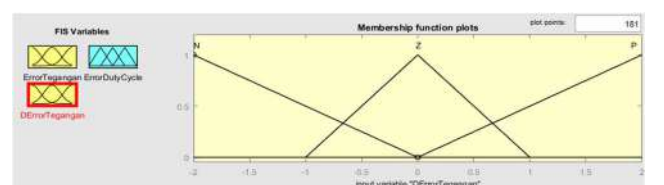


Fig 4. Membership functions input delta error voltage

- N (Negative) $\mu_N dE[y] : [-2 -2 0]$
- Z (Zero) $\mu_Z dE[y] : [-1 0 1]$
- P (Positive) $\mu_P dE[y] : [0 2 2]$

3) PWM Error Output Membership Function

The PWM Error Value is used to change the increase or decrease in the PWM value given to the MOSFET boost. The membership function in the PWM error output consists of three subsets, as follows:

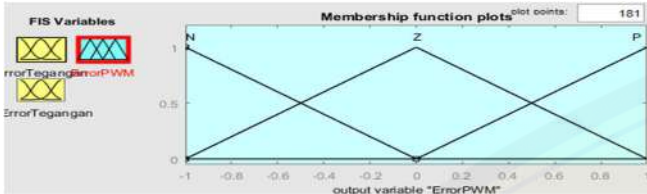


Fig 5. PWM error output membership function

- N (Negative) $\mu_N EPWM[z] : [-1 -1 0]$
- Z (Zero) $\mu_Z EPWM[z] : [-1 0 1]$
- P (Positive) $\mu_P EPWM[z] : [0 1 1]$

4) Fuzzy Model Inference Formation

This fuzzy model inference is formed based on the membership of each input so as to produce a decision in the form of output in the inference table.

TABLE II. FUZZY MODEL INFERENCE

dE E	N	Z	P
N	N	N	N
Z	N	Z	P
P	P	P	P

5) Fuzzy Rule Formation

The fuzzy rule is formed based on the inference of the fuzzy model in table II. The formation of fuzzy rules uses the and then relationship.

1. If (ErrorTegangan is N) and (DErrorTegangan is N) then (ErrorPWM is N) (1)
2. If (ErrorTegangan is N) and (DErrorTegangan is Z) then (ErrorPWM is N) (1)
3. If (ErrorTegangan is N) and (DErrorTegangan is P) then (ErrorPWM is N) (1)
4. If (ErrorTegangan is Z) and (DErrorTegangan is N) then (ErrorPWM is N) (1)
5. If (ErrorTegangan is Z) and (DErrorTegangan is Z) then (ErrorPWM is Z) (1)
6. If (ErrorTegangan is Z) and (DErrorTegangan is P) then (ErrorPWM is P) (1)
7. If (ErrorTegangan is P) and (DErrorTegangan is N) then (ErrorPWM is P) (1)
8. If (ErrorTegangan is P) and (DErrorTegangan is Z) then (ErrorPWM is P) (1)
9. If (ErrorTegangan is P) and (DErrorTegangan is P) then (ErrorPWM is P) (1)

Fig 6. Fuzzy rules

C. Flowchart Konverter

Based on Fig. 7 above, the system begins with the initialization of some of the components used such as the DC voltage sensor, ACS712 current sensor, fuzzy set or fuzzy member function, fuzzy rule or rule, PWM buck-boost variable and PV power variable. Then the readings of the voltage and current sensors are carried out at the output of the photovoltaic system (V_{pv} and I_{pv}), at the output of the converter system (V_{beban} and I_{beban}) and on the battery (V_{bat} and I_{bat}). After that, the parameters that have been read and initialized are displayed on the 20x4 LCD. Before going to the decision, the calculation of PV power is first carried out using the parameters of PV voltage and PV current.

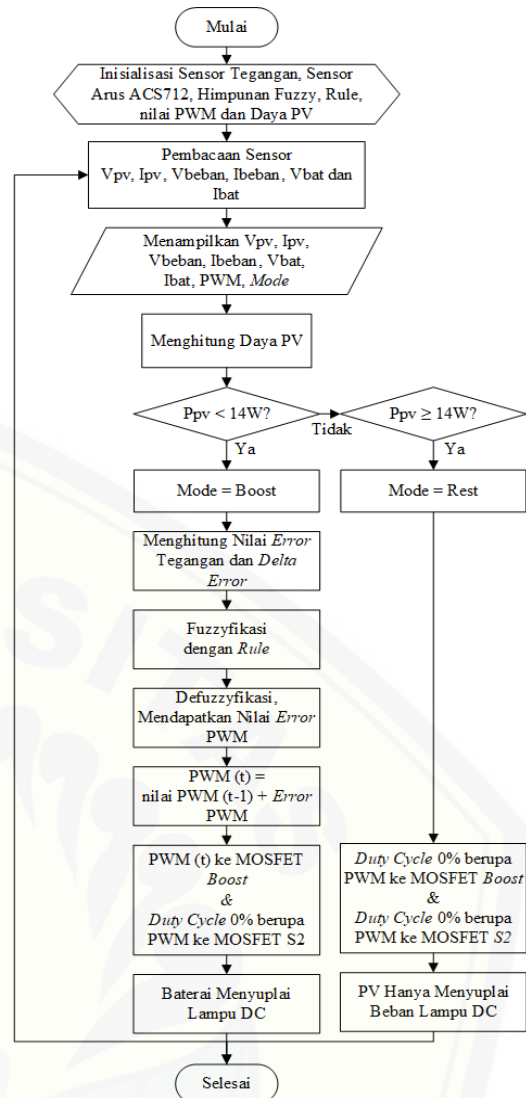


Fig 7. flowchart system DC-DC boost converter

There are two decisions that determine the work of the converter mode, namely boost and rest. The first decision is the boost mode, if the P_{pv} value is smaller than 14W, the mode variable will be given a string value that is "Boost", and then the fuzzy process starts. This fuzzy process starts by calculating the voltage error value and the voltage error delta value, then using the rule that has been made defuzzy to get the PWM error value. The PWM value of this fuzzy result is accumulated into the PWM value given to the MOSFET driver to control the work of the MOSFET boost. While the MOSFET S2 is signalled PWM 0 or inactive, so the battery supplies power to the DC lamp load.

The second decision is rest mode, if the P_{pv} value is greater than 14W, the mode variable will be given a string value, namely "Rest". In this mode, the BOOST MOSFET is signalled PWM 0 or inactive, so the PV only supplies the DC light load while the battery is on standby.

D. Data Testing

1) Voltage and Current Sensor Testing

Testing of voltage sensors using DC voltage sensors by comparing them using a wattmeter as a conventional measuring tool. Testing the current sensor using the ACS712 current sensor by comparing it using a wattmeter as a conventional measuring tool.

2) PWM testing

This PWM test is performed using an oscilloscope to determine the magnitude of the PWM signal generated by the PWM control circuit. This PWM control circuit consists of an Arduino Mega 2560 and a MOSFET driver.

3) Boost Mode Testing

Boost mode testing is carried out by providing an input voltage from the power supply from the boost side and then measuring the output voltage of the converter system with the PWM value of the accumulated fuzzy logic method Mamdani given to the MOSFET via the MOSFET driver.

E. Data Acquisition

1) Data Acquisition Of Rest-Boost Mode Converter

Data retrieval of the boost mode converter includes voltage and current on PV, load and battery with converter mode change from rest mode to boost mode with a predetermined time that is from 13:49 to 15:31.

2) Rest-Boost Mode Converter Power Calculation

The power calculation is done using the boost mode converter data parameters that read the voltage and current from the PV, load and battery which are then calculated into power parameters.

III. DATA ANALYSIS

This chapter discusses the design of the converter, testing and data retrieval results from the converter design, test plan and data acquisition plan in the previous chapter. Some of the main things that have been planned, then an analysis is carried out related to the method used.

A. System Design Result

1) Converter Circuit Design Result

The converter circuit is designed according to the component values that have been calculated in the converter design. This converter range consists of three 2-pin terminals, two 3-pin terminals, a 356µH inductor, a 100µF 50V capacitor, a 220µF 50V capacitor, two N-Channel IRF540N MOSFETs, and two MUR1560 diodes, see [4].

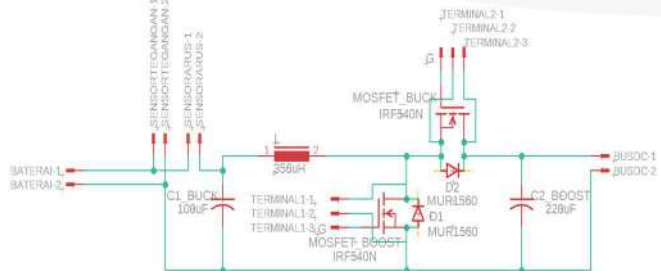


Fig. 8. Converter circuit

2) MOSFET Driver Circuit Design Results

The MOSFET driver circuit is designed based on the working voltage of the IRF540N MOSFET between 10V to 20V. Because of the use of two IRF540N MOSFETs, the MOSFET drivers made are a pair or two drivers. A DRIVER MOSFET consists of three 2-pin terminals, a TLP350 IC, a 1kΩ resistor, a 22Ω resistor, an LED, a 100nF 50V capacitor, and a MUR1560 diode. The TLP 350 IC works at voltages of 15V to 30V with an output voltage on pin 6 or Vo of about 13.6V when high and about -14.9V when low, so it is used in the declaration of the IRF540N MOSFET, see [5].

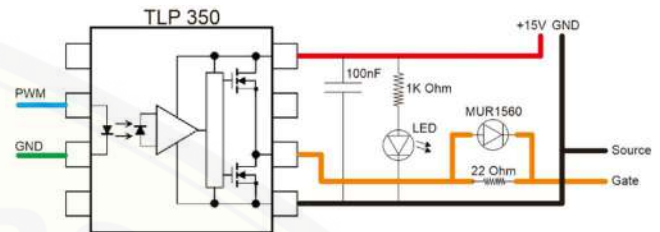


Fig. 9. MOSFET driver circuit

3) DC Bus Design Results

The DC bus is designed to make it easy to connect three important systems, namely the photovoltaic system, the DC-DC boost converter system and the 12V DC light load. The DC bus consists of five 2-pin terminals connecting the PV system, converter, load, ACS712 5A current sensor measurement and DC voltage sensor measurement.

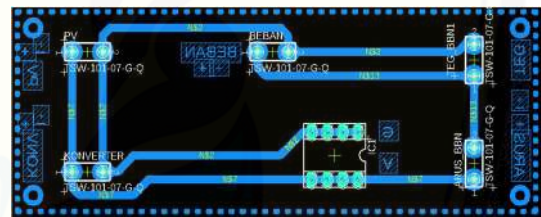


Fig. 10. DC Bus

4) Overall Circuit Design Results

The overall circuit is a combination of the converter circuit, MOSFET driver circuit, DC bus, microcontroller circuit, and other supporting components. Schematically, the overall circuit can be seen in Fig. 11 below.

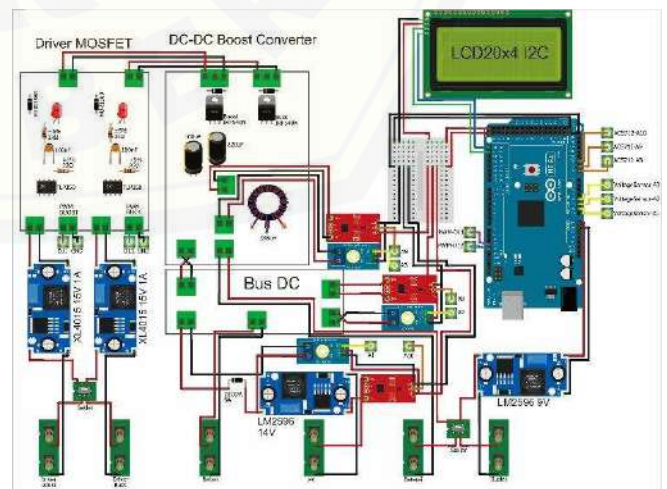


Fig. 11. Overall circuit scheme

From the overall circuit scheme, it has been realized into a series of DC-DC boost converter systems such as Fig. 12 as follows.

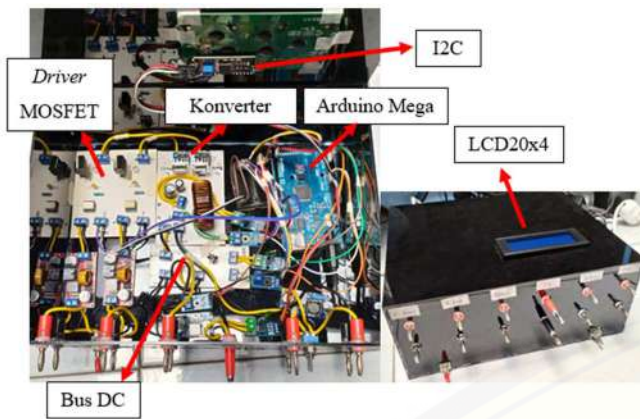


Fig 12. The Whole Set of Systems

The overall circuit of this system is designed based on the overall circuit scheme with supporting components of the MOSFET driver, namely the XL4015 Module which is used to regulate the supply voltage of the TLP350 IC by 15V and the current by 1A. The MOSFET driver work is turned on using the MTS202 toggle switch with three pairs of pins for two MOSFET drivers. Then four heatsinks are also used as supporting components, two heatsinks are used on the IRF540N MOSFET and two heatsinks are used on the MUR1560 diode on the MOSFET driver. In THE MOSFET driver, the use of the TLP350 IC is paired with an 8-pin IC socket which is useful in the maintenance of the MOSFET driver, making it easy to replace the IC in case of damage. The power jack is also used as the Arduino Mega 2560 supply replacing the LM2596 connection connected to the "Vin" and "GND" pins on the Arduino Mega 2560. A 6-pin toggle switch is also used to set the flame of the Arduino Mega 2560 and the relationship of the converter system to the lead acid battery.

From the converter design that has been done, the DC-DC boost converter system is designed with the following specifications.

TABLE III. DC-DC BOOST CONVERTER SPECIFICATION

Component	Specification
MOSFET IRF540N	100V 33A
Inductor	356μH
Capacitor S2	100μF / 50V
Capacitor Boost	220μF / 50V
Dioda MUR1560	15A 600V
Switching Frequency	20KHz
MOSFET Driver	IC TLP350 15V

B. Data Testing Results

1) Voltage and Current Sensor Testing

The sensor test consists of a voltage sensor and an ACS712 current sensor, which is carried out simultaneously, comparing the voltage sensor and the ACS712 current sensor with the conventional measuring instrument that is the Wattmeter.

TABLE IV. VOLTAGE SENSOR TESTING

No.	Wattmeter (V)	DC Voltage Sensor (V)	Error Percent (%)
1.	12.50	12.49	0.08
2.	12.50	12.51	0.08
3.	12.50	12.46	0.32
4.	12.50	12.54	0.32
5.	12.50	12.51	0.08
6.	12.50	12.49	0.08
7.	12.50	12.51	0.08
8.	14.00	14.05	0.36
9.	14.00	14.02	0.14
10.	14.00	13.95	0.36
11.	14.00	13.99	0.07
12.	14.00	14.02	0.14
13.	14.00	14.00	0.00
14.	14.00	13.98	0.14
15.	14.00	14.02	0.14
Average			0.16

After testing the voltage sensor, data from the voltage sensor test results in table IV used two voltage variations, namely 12.5V and 14V, which were adjusted to conventional Wattmeter tools. From fifteen test data, an average percent error value of 0.16% was obtained.

TABLE V. ACS712 CURRENT SENSOR TESTING

No.	Wattmeter (A)	ACS712 Current Sensor (A)	Error Percent (%)
1.	0.72	0.73	1.39
2.	0.73	0.73	0.00
3.	0.72	0.73	1.39
4.	0.71	0.73	2.82
5.	0.77	0.78	1.30
6.	0.78	0.77	1.28
7.	0.78	0.76	2.56
8.	0.77	0.78	1.30
9.	0.78	0.78	0.00
10.	0.79	0.78	1.27
11.	0.79	0.80	1.27
12.	0.76	0.78	2.63
13.	0.76	0.73	3.95
14.	0.77	0.78	1.30
15.	0.77	0.78	1.30
Average			1.58

After testing the ACS712 current sensor, the data from the voltage sensor test results were obtained in table V. From fifteen test data, the highest percent error value was 3.95% and the average percent error value was 1.58%.

2) PWM testing

PWM testing is performed using an oscilloscope by connecting the hook probe (positive) to the Vo or G (Gate) output of the MOSFET driver and connecting the crocodile probe (negative) to the GND or S terminal (Source). PWM testing was carried out eleven times using eleven data from duty-cycle 0% to 90% with an increase of 10% and the eleventh data of 96.78%.

From the PWM tests that have been carried out, the average test percent error value was 1.481% with the highest percent error value of 4.76% at 10% duty-cycle.

TABLE VI. PWM TESTING

No.	Duty Cycle (%)	PWM Value	Oscilloscope (%)	Error Percent (%)
1.	0	0	0%	0
2.	10	25.5	9,524%	4,76
3.	20	51.0	19,355%	3,225
4.	30	76.5	30,158%	0,527
5.	40	102.0	41,269%	3,173
6.	50	127.5	50,793%	1,586
7.	60	153.0	60,317%	0,528
8.	70	178.5	69,841%	0,227
9.	80	204.0	80,0%	0
10.	90	229.5	92,0%	2,222
11.	96,78	246.8	96,825%	0,046
Rata - Rata				1,481

3) Boost Mode Test Results

Boost mode testing is carried out by providing input voltages derived from the power supply with voltage variations, namely 9V, 10V, 11V, 12V and 13V, then the output voltage of the boost mode system is obtained which is taken when the system output voltage is stabilized by the given PWM value.

TABLE VII. BOOST MODE TESTING RESULT

No.	Power Supply	Voltage (V)		PWM	Error Percent (%)
		Boost	Calculation		
1	13.00	14.04	14.49	26.16	3.08
2	13.00	14.01	14.48	26.02	3.23
3	13.00	13.99	14.48	25.99	3.35
4	12.00	14.06	14.51	44.05	3.07
5	12.00	14.01	14.50	43.94	3.37
6	12.00	14.04	14.50	44.01	3.19
7	11.00	14.14	14.77	65.06	4.25
8	11.00	14.11	14.76	64.91	4.38
9	11.00	14.04	14.74	64.73	4.76
10	10.00	13.99	14.58	80.06	4.02
11	10.00	14.01	14.58	80.14	3.93
12	10.00	14.04	14.58	80.06	3.68
13	9.00	14.01	14.71	98.98	4.76
14	9.00	14.09	14.72	99.06	4.26
15	9.00	13.99	14.71	99.02	4.92
Average					3.88

From the boost mode tests that have been carried out, a comparison graph can be made between the power supply voltage and the boost output voltage to the PWM value as follows.

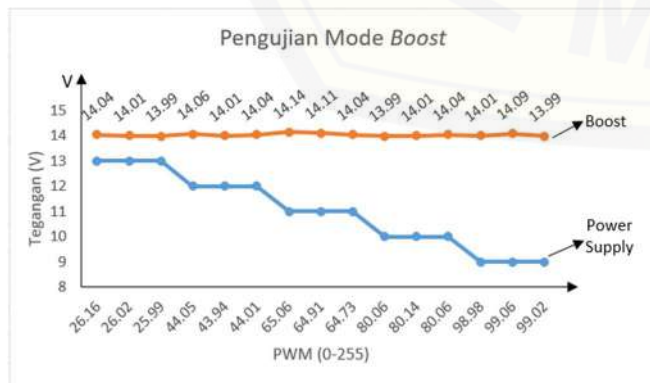


Fig. 13. Boost mode testing graphics

It can be seen that the input voltage coming from the power supply varies from 13V, 12V, 11V, 10V and 9V with 3 pieces of test data each. This test data is taken when the boost output voltage has stabilized with the given PWM boost value. It can be seen that the boost output voltage on the entire power supply voltage variation is stable between 13.99V to 14.14V. The calculation in theory is also carried out by calculating the power supply voltage with the measured PWM boost value using the boost converter equation. There was a percent error between the boost voltage and the theory calculation with an average of 3.88%.

C. Data Acquisition Results

1) Data of Rest-Boost Converter Mode

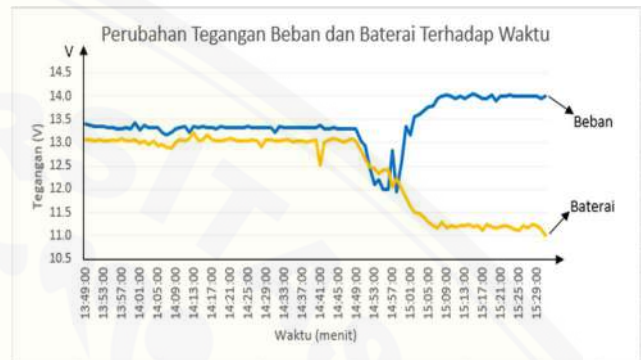


Fig. 14. Voltage against time graph

At 13:49 to 14:52, the rated load voltage is stable with a voltage rated range between 12.50V to 13.43V when the converter is in rest mode. Under these conditions, the photovoltaic system supplies the load of the DC lamp. While at the same hour, the battery voltage is rated in the range of 12.48V to 13.21V.

At 14.53 to 15.31, there was a voltage increase in the load from 11.94V to 14.06V, while there was a voltage drop in the battery with a range of 12.43V to 11.01V. This condition is caused by changing the rest mode to boost mode so that the photovoltaic system no longer supplies the dc light load, but the battery becomes a power source for the load. When the converter is in boost mode, there is a time when the converter returns in rest mode at 14:56. In boost mode, fuzzy works to generate a PWM signal which is used to turn on the declaration of the IRF540N MOSFET to produce an output voltage of 14V.

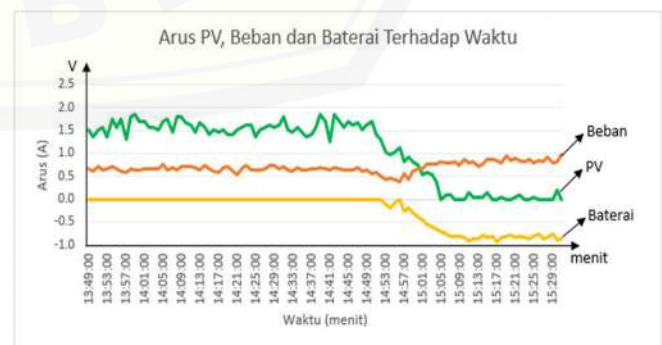


Fig. 15. Graph of current against time

The load current rated during data retrieval of the rest-boost mode converter is measured with a current range from 0.50A to 0.77A from 13.49 to 14.52, then undergoing a change from 14.53 to 15.31. The rated load current value increases with a current range of 0.37A to 0.98A when boosting mode.

The battery current reads 0A from 13.49 to 14.52, this state indicates that the battery is in standby condition when the converter is in rest mode and the PV is still capable of supplying load power. Then the second part is seen a decrease in the current value of the battery with a current range of 0A to -0.95A, this decrease to a minus or negative value is read, due to the current coming out of the lead acid battery, indicating that the converter is in boost mode so that the DC lamp load is supplied by the battery.

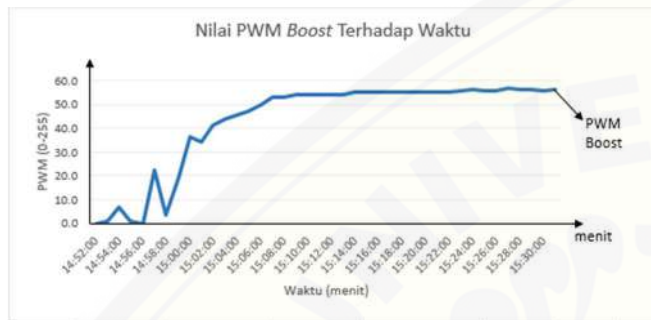


Fig. 16. Change graph of PWM value against time

During data retrieval, the PWM boost value is set by the accumulated PWM error value generated from the fuzzy method. The increase or decrease in the value of the PWM boost every 0.5 seconds is a maximum of 1. The change in the PWM boost value starts at 14:53 with the initial PWM boost value of 0.67. At 14:54 to 14:59, the PWM boost value looks up and down, this state is caused that within five minutes of data retrieval, the converter mode undergoes an unstable change from rest to boost and boost to rest caused by PV still able to meet the load power. Then starting at 15.00, the PWM boost value experienced a steady increase with an insignificant decrease, this state indicates the accumulated PWM boost value carried out by Arduino is working well, the system is able to set the PWM boost value with a voltage reference of 14V.

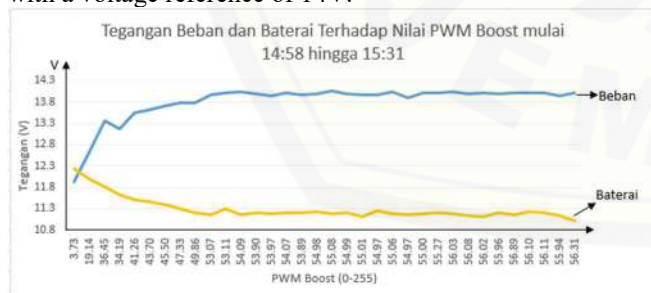


Fig 17. Comparison graph of load voltage and battery against PWM boost value

The boost mode optimally starts at 14:58, in this time range the PWM boost value increases due to the accumulation of PWM values from the fuzzy logic output of Mamdani. The increase in the load voltage is caused by the work of the boost mode converter which increases the output voltage according to the PWM boost value given to the

IRF540N boost MOSFET. The rated load voltage reached a reference voltage of 14V at 15.08 of 14.01V with a battery voltage of 11.49V, a PWM boost value of 53.11 or a duty-cycle of 20.827%. After reaching the reference voltage, the average load voltage during the boost mode is calculated at 13.99V with a voltage range from 13.89V to 14.06V.

2) Rest-Boost Mode Converter Power Data

The power data of the rest-boost mode converter is obtained from the calculation of the voltage and current that has been obtained in the rest-boost mode converter data collection table. This converter power data consists of photovoltaic system power, DC lamp load power, and lead acid battery power as well as converter mode from 13.49 to 15.31. Converter power data is needed to determine the response of changes in the DC-DC boost converter mode to changes in the power generated by the photovoltaic system.

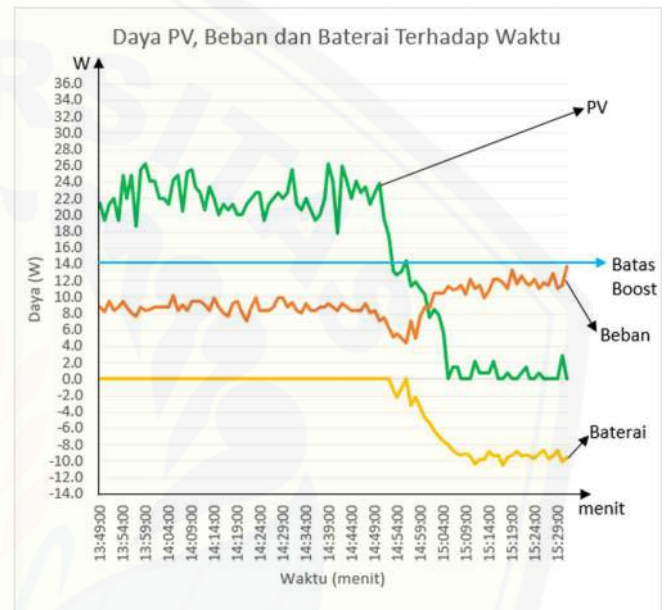


Fig. 18. Comparison graph of PV power, load and battery against time

Battery power in the time range from 13:49 to 14:51, the battery power is calculated to be worth 0W which indicates the battery is on standby. Then at 14:53, the battery power begins to be negative, this state indicates that the battery is in use. In this condition, the PV power seen on the chart is below the blue limit or boost mode limit with PV power calculated at 13.18W. Then when the PV power is calculated at 14.45W at 14.56, the battery power is calculated at 0W, in this condition the converter is in rest mode, and the PV system only supplies the DC light load while the battery is on standby. Then from 14:57 to 15:31, pv power continues to decrease with a decreased range from 11.85W to 0W causing the converter to be in boost mode, in this time range the battery power that comes out continues to increase, or in the graph continues to decrease because the negative value indicates that the battery supplies the load of the DC lamp.

As can be seen from Fig. 18, the calculated load power changes over time. This change is divided into two parts, namely at 13:49 to 14:51 or when the converter is in rest mode, and at 14:52 to 15:31 or when the converter is in boost mode. In the first section, it looks like the load power is calculated with a power range from 6.25W to 10.26W.

Then in the second part, the load power decreased with the lowest power of 4.44W at 14.56, then experienced an increase with a load power range of 5.01W to 13.73W. From the load power seen in the 4.43 chart, the converter system manages to keep the load supplied when the PV power is calculated below the boost mode set point of 14W.

IV. CONCLUSION

From the research that has been carried out, several conclusions can be obtained from the problems formulated, as follows.

1) DC-DC boost converter was successfully designed by calculating the selection of components, namely using $100\mu\text{F}$ s2 capacitors, $220\mu\text{F}$ boost capacitors, $356\mu\text{H}$ inductors, MUR1560 15A 600V diodes, and using IRF540N 33A 100V MOSFETs. This converter system works well in boost mode with an average percent error of boost mode testing of 3.88%.

2) The DC-DC boost converter system successfully uses the battery to keep the power to the load supplied. This is evidenced by the converter working well in boost mode, it can be seen in the data table of the rest-boost mode converter from 15.07 to 15.31 which shows a decrease in the battery voltage, but the output voltage of the converter is stable in the voltage range of 13.89V to 14.06V from the reference voltage which is 14V. At the same time, the load power is maintained in the power range of 9.91W to 13.73W.

3) The fuzzy logic used successfully provides output in the form of PWM error values which are accumulated into PWM boost values. This accumulated PWM value is given to the MOSFET through the MOSFET driver. The DC-DC boost converter system successfully raises the battery voltage from 11.94V to 13.79V with an increase in the PWM boost value from 3.73 to 49.86 for 8 minutes and maintains the stability of the boost output voltage in the voltage range of 13.89V to 14.06V using a PWM value range of 53.07 to 56.89 with a reference voltage of 14V.

V. REFERENCES

- [1] Firdaus, A.Z. Ahmad. Design and Simulation of Fuzzy Logic Controller for Boost Converter in Renewable Energy Application. *Jurnal Ilmiah*. Universitas Malaysia Perlis. 2013.
- [2] Kusuma Wijaya, Yudo. Desain dan Implementasi Konverter DC-DC Buck Boost Dua Arah untuk Aplikasi Kendaraan Listrik. *Technology Institute of Sepuluh Nopember*. 2015.
- [3] Sukma Pratiwi, Armadilla. Desain dan Simulasi Bidirectional DC-DC Converter untuk Penyimpanan Energi pada Sistem Fotovoltaik. *Jurnal Nasional Teknik Elektro dan Teknologi Informasi*. 2020.
- [4] Sulistomo, Pinandito. Implementasi Pengendalian Sistem Pengisian/Pengosongan Baterai pada Sistem Photovoltaic Stand-Alone Menggunakan Bidirectional Converter dengan Metode Proportional-Integral Berbasis Mikrokontroler DSPIC30F4011. *Script*. Universitas Diponegoro. 2018.
- [5] V., Viswanatha. Microcontroller Based Bidirectional Buck-Boost Converter for Photo-voltaic Power Plant. *Scientific Journals*. Department of Electrical and Electronics Engineering, REVA University. 2017.